WM2008 Conference, February 24-28, 2008, Phoenix, AZ
Abstract #8170

Computational Fluid Dynamics Best Practice Guidelines in the Analysis of Storage Dry Cask

A Zigh, J Solis
US Nuclear Regulatory Commission
11545 Rockville Pike, Rockville, MD 20852
MS-T10K08

ABSTRACT

Computational fluid dynamics (CFD) methods are used to evaluate the thermal performance of a dry cask under long term storage conditions in accordance with NUREG-1536 [NUREG-1536, 1997]. A three-dimensional CFD model was developed and validated using data for a ventilated storage cask (VSC-17) collected by Idaho National Laboratory (INL). The developed Fluent CFD model was validated to minimize the modeling and application uncertainties. To address modeling uncertainties, the paper focused on turbulence modeling of buoyancy driven air flow. Similarly, in the application uncertainties, the pressure boundary conditions used to model the air inlet and outlet vents were investigated and validated. Different turbulence models were used to reduce the modeling uncertainty in the CFD simulation of the air flow through the annular gap between the overpack and the multi-assembly sealed basket (MSB). Among the chosen turbulence models, the validation showed that the low Reynolds k-ε and the transitional k-ω turbulence models predicted the measured temperatures closely. To assess the impact of pressure boundary conditions used at the air inlet and outlet channels on the application uncertainties, a sensitivity analysis of operating density was undertaken. For convergence purposes, all available commercial CFD codes include the operating density in the pressure gradient term of the momentum equation. The validation showed that the correct operating density corresponds to the density evaluated at the air inlet condition of pressure and temperature. Next, the validated CFD method was used to predict the thermal performance of an existing dry cask storage system. The evaluation uses two distinct models: a three-dimensional and an axisymmetrical representation of the cask. In the 3-D model, porous media was used to model only the volume occupied by the rodded region that is surrounded by the BWR channel box. In the axysymmetric model, porous media was used to model the entire region that encompasses the fuel assemblies as well as the gaps in between. Consequently, a larger volume is represented by porous media in the second model; hence, a higher frictional flow resistance is introduced in the momentum equations. The conservatism and the safety margins of these models were compared to assess the applicability and the realism of these two models. The three-dimensional model included fewer geometry simplifications and is recommended as it predicted less conservative fuel cladding temperature values, while still assuring the existence of adequate safety margins.

INTRODUCTION

Dry storage cask designs for spent nuclear fuel are submitted to the U.S. Nuclear Regulatory Commission (NRC) for certification under 10 CFR 72. Technical review of these design applications is performed in accordance with 10 CFR 72 and the "Standard Review Plan for Dry Cask Storage Systems" (NUREG-1536, SRP). To ensure that the temperatures of the cask, fuel cladding, and fuel remain within allowable values, a thermal review of the application is performed. Recent design applications have increasingly utilized thermal-hydraulic analyses and CFD codes (e.g., Fluent), to demonstrate the adequacy of the design. Peak cladding temperatures could be underpredicted if best practice guidelines for CFD are not followed.

***The opinions expressed in this paper are strictly those of the authors and do not constitute official U.S. Nuclear Regulatory Commission position.

This paper addresses two categories of uncertainties, with specific guidelines to minimize them. The first category is modeling uncertainties. These uncertainties are due to the difference between the real flow and the approximate solution of the model equations. This paper provides an independent verification and validation of the modeling approach used to model the heat transfer and fluid flow in a dry cask to reduce modeling uncertainties. In particular, the discussion of modeling uncertainties focused on the turbulence modeling which can greatly influence the final results if not applied correctly. Fluent has many turbulence models that are not generalized and, therefore, can not be applied to all types of flows. Depending on the complexity of the flow, some models are more suited than others. In this paper, several approaches to model air flow turbulence have been investigated and compared to experimental data. The paper suggests CFD best practice guidelines to minimize turbulence modeling uncertainties in the dry cask analysis.

The second category of uncertainty is the application uncertainties. These uncertainties are introduced because the application is complex and precise data needed for the simulation is not always available. In this paper, the discussion of application uncertainties focused on the inlet and outlet boundary conditions of cooling air. In a ventilated dry cask, as cooling air is naturally induced, pressure boundaries were the preferred choice at the air inlet and outlet ducts. The pressure gradient in the air flow channel affects the magnitude of the potential buoyancy forces due to the heat source (i.e. decay heat) and as such, these pressure boundary conditions are very crucial to the uncertainties that can be introduced in the simulation. In this paper, the effect of the pressure boundary conditions was investigated and compared to the experimental data to minimize the application uncertainties. This paper gives specific guidelines to avoid application uncertainties that could arise in the specification of the pressure boundary conditions at the air inlet and outlet ducts of the dry cask.

This study consisted of two phases. The first phase was a validation of the method. This step ensured that the CFD model being solved is a good representation of the cask design. Experimental data previously obtained for a ventilated storage cask were used for the validation. To reduce modeling uncertainties, different turbulence models were used and compared to the experimental data. The low Reynolds k-ε turbulence model was found to give very satisfactory results. To reduce the application uncertainties, sensitivity analyses using different pressure gradients by varying the operating density were performed. Comparison to the experimental data showed that the correct operating density corresponded to the density evaluated at the air inlet conditions of pressures and temperatures. The second phase of the study included the application of the validated method to model a storage cask holding 68 Boiling Water Reactor (BWR) assemblies under normal storage conditions. Two methods were used to model this particular dry cask to investigate the degree of conservatism of the obtained results. The first method used an axisymmetrical model to represent flow and heat transfer in the dry cask. The second method used three-dimensional geometry to perform the analysis. The difference between the 3-D models is the extent of the volume represented by porous media. The results demonstrated that the bigger the porous media volume is; the more conservative the results will be. The axisymmetrical approach led to conservative results. The 3-D model has the least volume that uses porous media modeling and, as such, it is more realistic and is recommended.

Porous media is used to model flow through fuel assemblies to save both CPU time and modeling effort. In the porous media assumption, fuel rods are replaced by an equivalent flow resistance (frictional and inertial) and an effective thermal conductivity. The flow regime for air flow and helium flow is another important parameter that can affect the analysis. The assumption of fully turbulent flow inside and outside the canister, will lead to a lower Peak Cladding Temperature (PCT). On the other hand, assuming laminar flow inside and outside the canister would lead to a higher PCT. As such, careful and correct

characterization of the flow regime is required to avoid misprediction of the flow variables. In the present analysis, different turbulence models were used to model the air flow in the dry cask cooling channel. Four models were used covering the low and high range of Reynolds number as well as the transitional range. In addition to standard k-ε model and laminar flow models, low Reynolds k-ε, and transitional k-ω Shear Stress Transport (SST) models were used. The standard k-ε model is suited to model high Reynolds fully-developed turbulent flows, while low Reynolds k-ε and transitional k-ω SST models are adequate to model flows in low, transitional, and high Reynolds range.

Pressure boundaries are used to model heat and flow in the dry cask. One issue that arose while using pressure boundary conditions at the inlet and exit of the dry cask is the operating density. This parameter has major effect on the results, and should be used properly. To assess the use of the pressure boundary conditions, two types of control volumes were used to perform the analysis. One choice was to include part of the outside ambient to the dry cask. Hence, the inlet and outlet vents will not be part of the specified boundary. Instead, the inlet and outlet channels will be part of the computational domain. In the second choice, the boundaries of the cask were used as a boundary of the modeled control volume. At the start, the first control volume results were used to validate the inlet boundary conditions (i.e. inlet temperature) to the second control volume. Operating density is an input parameter to Fluent and will be of great importance to the final results when pressure boundaries are used as shown in [Fluent, 2006]. According to the Fluent user manual, the operating density should be representative of the volumetric average density of the fluid. In the extended control volume, the air volume consists, in big part, of the chosen isothermal ambient volume and the negligible volume of air cooling the canister in the air duct between the canister and liner walls. Therefore, for the extended control volume case, the operating density will be equal to that of the ambient. When the second control volume is chosen, the volume of the air consists of only the air flowing in the air duct which is getting warmed as it goes up. According to [Fluent, 2006], the operating density in this case is equal to the volumetric average density of the column of air between the inlet and the outlet ducts.

PART I (Validation)

Description of the VSC-17 Spent Fuel Storage Cask Experiments

The VSC-17 spent fuel storage system is a passive heat dissipation system for storing 17 assemblies of consolidated spent nuclear fuel. The VSC-17 system consists of a ventilated concrete cask (VCC) enclosing a multi-assembly sealed basket (MSB) containing spent nuclear fuel as shown in Figure 1. Decay heat generated by the spent fuel is transmitted through the containment wall of the MSB to a cooling air flow. Natural circulation drives the cooling air flow through an annular path between the MSB wall and the VCC liner wall and carries the heat to the environment without undue heating of the concrete cask. The annular air flow cools the outside of the MSB and the inside of the VCC.

The performance testing consisted of loading the MSB with 17 fuel cans containing consolidated Pressurized Water Reactor (PWR) spent fuel from Virginia Power's Surry reactors and Florida Power & Light's Turkey Point reactors. At the time of the cask tests, this fuel was generating about 14.9 kW decay heat. Temperatures of the cask surface, concrete, air channel surfaces, and the fuel compartments (containing the fuel cans) were measured. Testing was performed with vacuum, nitrogen, and helium backfill environments in a vertical cask orientation, with air circulation vents open, partially blocked, and completely blocked. Of these tests, Run #1 (no blocked vents) with helium gas in the MSB was chosen for validation. Detailed descriptions of the VSC-17 experiments, including system geometry, instrumentation locations, specifics of fuel loading, and estimates of the heat generation rates in the spent fuel assemblies are included in the original documentation of the testing [McKinnon, 1992].

Decay Heat Generation (Thermal Source Term) for Consolidated Fuel Cans

Individual consolidated fuel cans in the VSC-17 had heat generation rates ranging from 0.707 kW to 1.05 kW. The fuel cans were loaded in the basket to give as close to a symmetrical heat load as possible, with fuel cans near 1.0 kW in the central 3x3 grid, and fuel cans with heat loads near 0.7 kW on the periphery of the basket as shown in [McKinnon, 1992]. Most of the temperature measurements obtained within the fuel cans and the basket are from thermocouples located in one quadrant of the basket. In this quadrant, the peripheral fuel cans all have decay heat values of approximately 0.744 kW, and the inner fuel cans have decay heat values ranging from 0.962 kW to 1.048 kW. The specific heat generation rates for these fuel cans were applied to the homogeneous regions modeling the corresponding fuel cans in a quarter symmetry representation of the MSB.

The decay heat for a given fuel can was applied as a uniform volumetric heat generation rate throughout the homogeneous region, modified only to include an axial power profile based on the measured axial power distribution in the fuel cans as shown in Figure 2. The heat generation is applied over 388 cm (153 inches). The actual heated length for this fuel is estimated at 145.5 inches (i.e., an original length of 144 inches, plus 1.5 inches of growth due to burn-up.) This approximation will result in slightly lower peak fuel temperature predictions than would be obtained if the shorter (actual) heated length were to be used. The consolidated fuel cans were modeled as non-porous solid using the effective thermal conductivities obtained from the 2-D fluent thermal model of a single assembly.

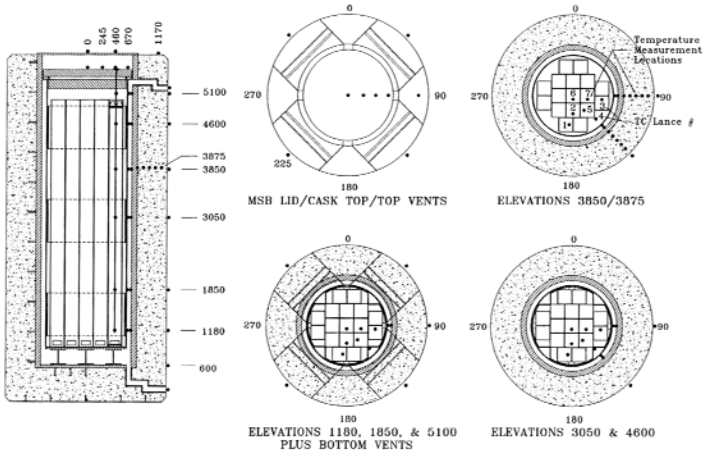

Figure 1 Temperature measurement locations for VSC-17

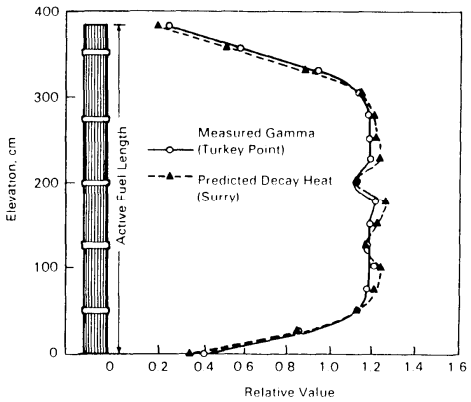

Figure 2 Axial decay heat profile

Cases Considered

At first, extended control volume (CV) was used. The control volume included the cask geometry as well as a portion of the surrounding ambient. Two cases using different number of cells were used to check for grid independent solution. The first grid consisted of 1.2 million cells while the second mesh had 2 million cells. In the finer mesh case, the additional cells were placed near the surrounding VCC and MPC walls, the air flow duct and walls surrounding inert gas flow regions inside the canister. Only the transitional SST k-ω model was used in this part of the analysis to model the turbulence in the air flow region. As pressure boundaries are used at the inlet and outlet boundaries, an input for operating density is required. As such, in this part of the analysis, cases were created to investigate the effect of operating density on the final results. Most of the analyses performed in this paper used the control volume that includes the dry cask body only without any additional surrounding ambient (i.e. smaller CV). To do so, initially the results obtained from the smaller CV and the extended CV were compared. This step was very important to the rest of the investigations, as the correct operating density for the smaller CV was

found. Also, in this part, the measured inlet temperature was checked for consistency. It was noticed through the experimental data, that the average temperature at the inlet was at least 13 degrees higher than the surrounding ambient temperature. This step was of utmost importance, due to the major difference that can be obtained in the final results when different inlet temperature boundary conditions were used. Different cases were run to investigate the influence of different temperatures at the inlet for the smaller CV. The effect of using different turbulence models was investigated using the smaller CV. Among the turbulence models available in Fluent, transitional k-ω SST, low Reynolds k-ε, and standard k-ε models were used to model the flow of air. Laminar model was also used due the low Grashof and modified Grashof in the duct as explained in [Sparrow EM et al., 1985].

Results and Discussions

Three turbulence models as well as a laminar regime were used to model the air flow passage between the MSB and the concrete liner. The first two models among the three chosen turbulence models were the transitional SST k-ω model and the low-Reynolds k-ε model. Both of these models use damping functions that take into account the effect of the cell Reynolds number on the calculation of the time and length scale of turbulence. Both of these models are used with a fine grid near the wall (y+ ~1) to enable integration through the viscosity-affected near wall region. The third chosen turbulence model was the standard k-ε in conjunction with standard wall function to bridge the fully turbulent core region to the viscosity-dominated region near the wall. This model does not use a fine mesh near the wall. In the present application a y+ close to 20 was used.

Temperature profiles resulting from CFD using the four approaches described above are compared to the experimental data. Axial temperature profile experimental data for different lances inside the fuel region, liner wall and MSB wall were chosen to compare to calculated CFD results. Additionally, radial profiles from the center of the fuel region to the periphery of the overpack concrete shield at two elevations (3.05 m and 3.85 m) were used to compare the experimental data to the CFD results. Initially, the extended control volume case was used. The studied volume included the cask geometry and a portion of the surrounding ambient. Two types of grids were used to check for grid independent solution. Only the transitional SST k-ω model was used in this part of the analysis to model the turbulence in the air flow region. Figures 3a through 3c show the CFD temperature distributions along with experimental data. Both grids resulted in the same temperature distribution and, as such, only results from one grid are shown in Figures 3a through 3c.

The extended control volume case was also used to find the appropriate operating density for the smaller CV model (i.e. dry cask only). Fluent user manual [Fluent, 2006] indicates that the operating density should be equivalent to the volumetric average density of the fluid. In the extended control volume, the air volume consists of the extensive ambient air and the air sandwiched between the liner and the MSB walls. As the volume of the hot air between liner and MSB walls is negligible compared the represented ambient volume, the average density is closer to the ambient density, and so is the operating density. When the chosen control volume consisted of only the dry cask, the air volume consisted of only the air between the VCC liner and the MSB walls. This air volume continuously removed heat from the MSB wall. As a result the temperature increases from the inlet to the outlet of the cask. The average fluid temperature of this modeled volume is higher than the ambient temperature, and as such, the operating density is lower. The VSC-17 without the ambient (i.e. smaller CV) used the first grid generated for the extended CV but without the cells to model the ambient. The average measured ambient temperature was used at the inlet duct of the smaller CV. The results for this simulation are shown in Figures 4a and 4b. The results were identical to the results obtained for the extended control volume shown in Figure 3a through 3c, indicating that the problem was correctly modeled (i.e. correct

operating density was chosen). The operating density used for this case corresponded to the inlet temperature and not the volumetric average as suggested by Fluent user guide manual [Fluent, 2006].

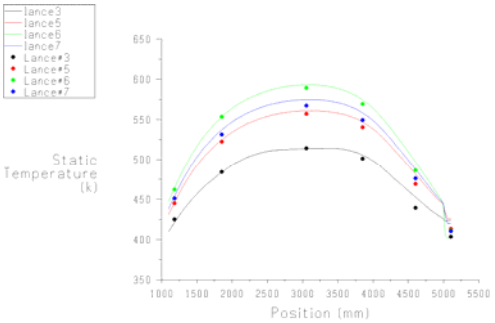

Figure 3a Fuel axial temperature for extended geometry and transitional k-ω SST turbulence model. (── CFD, ● Experiment).

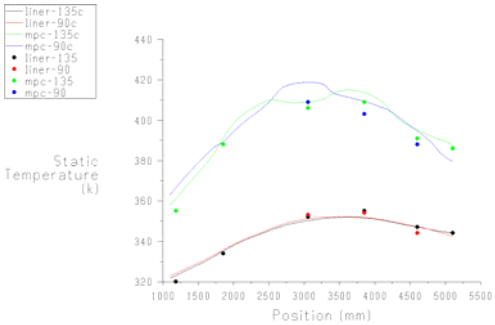

Figure 3b Liner and MSB walls axial temperature for extended geometry and transitional k-ω SST turbulence model. (── CFD, ● Experiment).

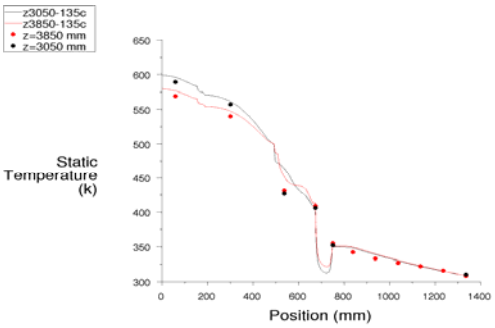

Figure 3c Radial temperatures at two axial locations using extended geometry and transitional k-ω SST turbulence model.(── CFD, ● Experiment).

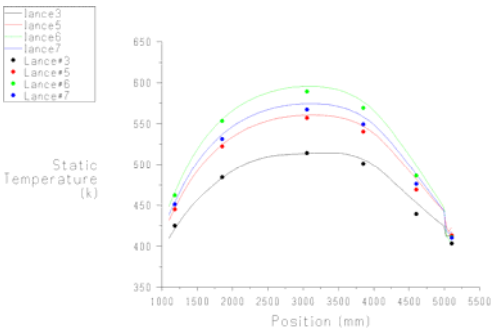

Figure 4a Fuel axial temperature using transitional k-ω SST turbulence model.
(── CFD, ● Experiment).

When the same case was run with the operating density as the average fluid density, the air mass flow entering VSC-17 was 50 % less and the exit air temperature was 12 degrees higher as shown in Table 1. Table 1 also indicates that less heat was absorbed from the fuel rods and the PCT temperature is higher. If a value for the operating density is not specified, Fluent will use the average density of all the modeled fluids. As in this case, it will use the volumetric average density of both air and helium. As helium density is much lower than air density for the given conditions, the volumetric average density will be even lower than the air volumetric average density. As such, lower air mass flow rate will be induced, and higher PCT will be obtained. The reported measured inlet temperature values were 12 degrees higher than the environment. There are no apparent reasons for the temperature at the inlet to increase. The data indicates an inlet average temperature of 35°C, yet the cask surface temperature just above the inlet is about 27°C. Either the thermocouples at the inlet were reading wrong measurements or they were affected by radiation from the inside of the cask. Either way, these thermocouples were apparently not measuring the correct temperature at the inlet duct of the dry cask. To settle this issue, in the extended CV CFD case, the inlet temperature is not part of the boundary conditions but it is part of the solved domain. Fluent results show that the temperature at the entry of dry cask is identical to the ambient temperature as shown in Table 2. Table 3 shows the exit temperature for the smaller CV using three different turbulence models. These cases used the average measured inlet temperature as the inlet temperature boundary. The turbulence models used are the low Reynolds k-ε model, the transitional k-ω

SST model and the standard k-ε. As shown in Table 3, all the three turbulence models led to the same higher temperature. The resulted exit temperature is 5 degrees higher than the measured average exit temperature.

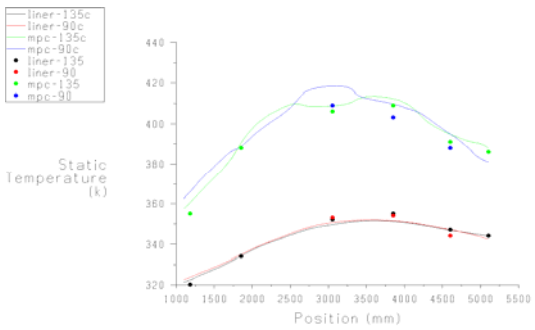

Figure 4b Liner and MSB Walls axial Temperature using transitional k-ω turbulence model. (──CFD, ● Experiment).

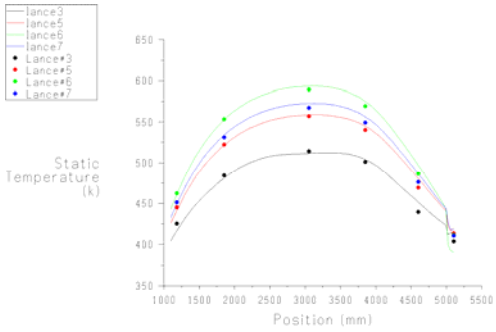

Figure 5a Fuel axial temperature using low Reynolds k-ε turbulence model. (── CFD, ● Experiment).

Table 4 shows the exit temperature for the smaller CV using three different turbulence models. These cases used the ambient temperature as an inlet temperature boundary condition. The turbulence models used are the low Reynolds k-ε model, the transitional k-ω SST model and the standard k-ε. As shown in Table 4, all the three turbulence models predicted very well the exit temperature for the smaller CV when compared to the experimentally obtained data. This is yet another proof and indication that the reported measured inlet temperature values do not correctly reflect a realistic inlet temperature. As a result the average measured ambient temperature was used as the inlet temperature for the smaller CV.

Figures 4a-4b, 5a-5b, 6 and 7 show the temperature distributions for different turbulence models. Transitional k-ω SST, low Reynolds k-ε, standard k-ε, and laminar flow regime were used respectively. The Figures respectively show the axial distribution of the fuel inside the canister, MSB and liner walls. As a first observation, all the four options used to model the turbulence in the air cooling channel were successful in predicting the location of the peak cladding temperature. The peak cladding temperature value is of great importance in dry cask applications. For long term normal storage conditions, peak cladding temperature is limited to 400°C to avoid fuel cladding deformation caused by excessive creep and to limit the amount of radially oriented hybrides [ISG-11].

Both, the transitional k-ω SST and the low Reynolds k-ε turbulence models predicted the temperature distribution fairly well in the fuel region inside the canister as well as the passage of cooling air (i.e. MSB and liner walls). Both Figure 4a and 5a show that these two models predicted the location and the value of the peak cladding temperature. Additionally the temperature axial profile of the liner wall and MSB wall were fairly well predicted given the complex nature of this buoyancy driven flow as shown in Figures 4b and 5b. The improvement in the prediction of the liner wall temperature distribution was the result of using a fine mesh near the walls and the capability of these two models to handle low Reynolds turbulent flow. Table 4 shows that when standard k-ε model is used, slightly higher air mass flow rate is induced, thus higher heat rate is absorbed from the cask resulting in a lower air exit temperature. Table 4 shows that when laminar regime is used, a lower air mass flow rate is induced. As a consequence lower heat is absorbed from the cask and higher PCT is predicted. The liner and the MSB wall axial temperature distributions were consistently higher than the experimental data when laminar regime was used as shown in Figure 7.

The Standard k-ε model was a better choice than the laminar option, but due to the lack of finer grids near the MSB wall and the liner wall, this model was unable to capture the temperature distribution at the liner wall. This model over-predicted the heat exchange between the two walls. Usually, standard k-ε model combined with standard wall function is used when high Reynolds number flow exists. However, this model is not suitable for transitional buoyancy driven flows. The standard k-ε model under-predicted slightly the MSB wall distribution and missed in predicting the liner wall axial distribution. As shown in Table 4 the standard k-ε model over-predicted the heat transfer from MSB wall to the liner, as a result lower temperature will be obtained on the liner wall. The reason behind this is that the standard k-ε is not well suited for low Reynolds number flow and transitional flows. Integration to the wall (i.e. finer grid near the wall) is required to get more information about the wall shear stress and heat transfer for low Reynolds number and transitional flows. In case of transitional Reynolds numbers, as in the case we are dealing with, some type of damping function to enable computation across the laminar viscous sub-layer is required in conjunction with fine mesh near the wall, as was done with the first two turbulence models chosen in this analysis. The standard k-ε under-predicted the liner wall axial temperature distribution as shown in Figure 6, for the reasons enumerated above. Figure 8 shows the outside surface axial temperature distribution using low Reynolds k-ε turbulence model. The CFD analysis followed the trend and predicted correctly the measured temperatures. This Figure shows how well the heat transfer and fluid flow was modeled radially.

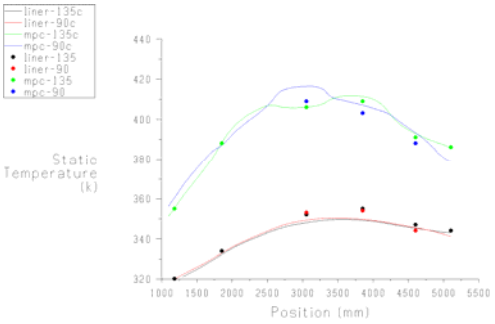

Figure 5b Liner and MSB walls axial temperature using low Reynolds k-ε turbulence model.
(—— CFD, ● Experiment).

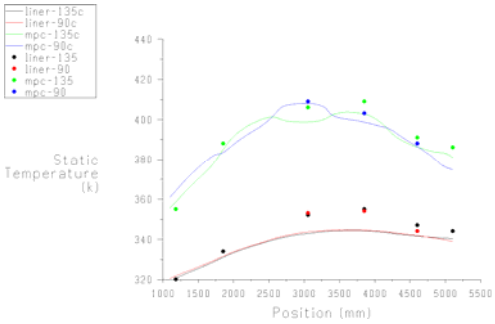

Figure 6 Liner and MSB walls axial temperature using standard k-ε turbulence model.
(—— CFD, ● Experiment).

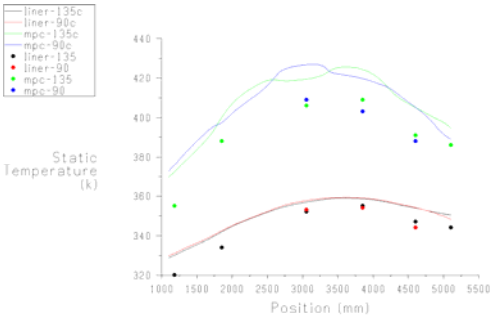

Figure 7 Liner and MSB walls axial temperature using laminar flow regime.
(—— CFD, ● Experiment).

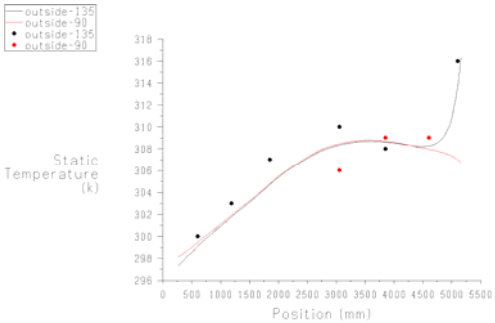

Figure 8 Outside surface temperature using low Re k-ε turbulence model.
(—— CFD, ● Experiment).

Test#	Operating density (kg/m3)	Peak cladding Temperature (Kelvin)	Air mass flow rate (kg/s)	Heat absorbed by air (Watts)	Air exit temperature (Kelvin)
Test #1	1 (inlet)	598	0.238	9,284	339
Test#1	0.92 (average)	607	0.1272	7,816	351

Table 1 3-D VSC-17 model with varying operating density

Control Volume	Turbulence model	Inlet average temperature (Kelvin)	Inlet max temperature (Kelvin)	Exit average temperature (Kelvin)	Exit max temperature (Kelvin)
Dry cask + Ambient	Transitional k-ω SST	296.2	296.8	335	340
Dry cask	Transitional k-ω SST	296.2	296.2	335	339
Dry Cask	Low Re k-ε	296.2	296.2	335	339
Dry cask	Standard k-ε	296.2	296.2	333	338
Dry cask	Laminar	296.2	296.2	335	352

Table 2 Inlet and outlet air temperature (Kelvin) for different turbulence models

Control Volume	Turbulence model	Inlet temperature (Kelvin)	Inlet max temperature (Kelvin)	Exit average temperature (Kelvin)	Exit max temperature (Kelvin)
Dry cask	Transitional k-ω SST	308	308	345	350
Dry Cask	Low Re k-ε	308	308	345	349
Dry cask	Standard k-ε	308	308	343	348

Table 3 Inlet and outlet air temperature for different turbulence models using higher inlet temperature

Control Volume	Turbulence model	Air mass flow rate (kg/s)	PCT (Kelvin)	Heat absorbed by air (Watts)	Air exit temperature (Kelvin)
Dry cask + Ambient	Transitional k-ω SST	0.235	599	9,300	335
Dry cask	Transitional k-ω SST	0.238	599	9,290	335
Dry Cask	Low Re k-ε	0.24	597	9,400	335
Dry cask	Standard k-ε	0.244	592	9,710	333
Dry cask	Laminar	0.201	606	8,630	335

Table 4 VSC-17 model using different turbulence models

PART II: (MPC-68 Thermal Analysis)

General Description of the Analyzed Cask System

The analyzed cask existing cask system consists of a sealed canister inside a vertical ventilated storage overpack as shown in Figure 9. Four air inlet ducts at the bottom of the cylinder overpack and four outlet ducts at the top are used to air-cool the stored Multi-Purpose Canister (MPC). The spent nuclear fuel (SNF) assemblies reside inside the MPC, which is sealed with a welded lid to form the confinement boundary. The MPC contains an all-alloy honeycomb basket structure with a square-shaped compartment of appropriate dimensions to allow insertion of the fuel assemblies prior to welding of the MPC. The MPC is backfilled with helium to provide a stable, inert environment for long-term storage of the SNF.

The helium fills all the space between the solid components and provides an improved conduction medium for dissipating decay heat in the MPC. Heat is rejected from the SNF in the dry cask system to the environment by passive heat transport mechanisms only.

The analyzed long term storage system is comprised of two discrete components: a multi-purpose canister (MPC) and storage overpack. The MPC is a welded cylindrical structure, consisting of a honeycombed fuel basket, a base-plate, canister shell, a lid and a closure ring. The number of spent nuclear fuel storage locations in each of the MPCs depends on the fuel assembly characteristics. The MPC confinement is constructed entirely from stainless steel alloy material. The overpack is a rugged, heavy-walled cylindrical vessel. The main structural function of the storage overpack is provided by carbon steel, and the main shielding function is provided by plain concrete. The overpack plain concrete is enclosed by cylindrical steel shells, a thick steel baseplate, and a top plate. The storage overpack provides an internal cylindrical cavity of sufficient height and diameter for housing an MPC.

Compliance of the system thermal performance with 10 CFR 72 requirements for outdoor storage at an ISFSI should be established. The analysis considers passive rejection of decay heat from stored SNF assemblies to the environment under normal conditions of storage. The effect of incident solar radiation (insolation) is included in the analysis. The system thermal evaluation follows the guidelines of NUREG-1536 [NUREG-1536, 1997] and Interim Staff Guidance Memorandum No. 11 (ISG-11) [ISG-11] to demonstrate thermal compliance of the system. These guidelines provide specific limits on the permissible maximum cladding temperature in the stored commercial spent fuel and other confinement boundary components, and on the maximum permissible pressure in the confinement space under certain operating scenarios.

In the present analysis, the system is evaluated for uniform loading, under normal storage, holding BWR assemblies. Every basket cell is assumed to be occupied with fuel producing heat at maximum rate. The analyzed dry cask system is designed for uniform decay heat of 34 kW, a helium backfill pressure of 7 atm, and normal ambient temperature.

Three Dimensional (3-D) Thermal Model

The interior of the MPC is a 3-D array of square cells inside an irregular shaped basket outline confined inside the cylindrical space of the MPC cavity. To ensure an adequate representation of these features, a 3-D geometric model of the MPC is constructed. Because, it is computationally very expensive, labor intensive and impractical, fuel rods are not individually modeled. Instead the cross section bounded by the inside of the channel box which surrounds the fuel rods and the interstitial helium gas, is replaced by an equivalent square homogeneous section characterized by an effective thermal conductivity and equivalent flow resistances. In the 3-D model the storage cell is divided into two distinct axial flow regions, namely, the in-channel (rodded) region and the annulus region between the channel box and the storage cell as shown in Figure 10. The composite walls in the fuel basket consisting of the steel structural panels, the aluminum-based neutron absorber, and the steel sheating, are represented by an orthotropic homogeneous panel of equivalent thermal conductivity in the three principal directions. The in-plane and thru-thickness thermal conductivities of the composite wall are computed differently.

The in-plane thermal conductivity of fuel assemblies is obtained using 2-D CFD analysis of an array of fuel rods enclosed by a square box as shown in Figures 11 for 3-D model. The energy conservation equation including radiation and conduction heat transfer is solved. The effective conduction-radiation conductivities are obtained for a given fuel rod heat source and isothermal boundary conditions. The final thermal conductivities of the rodded region, like the porous media simulation for helium flow, are

represented by a 3-D continuum having effective planar and axial conductivities. The internals of the MPC, including the basket cross section, bottom mouse holes, top plenum, and circumferential irregular downcomer are modeled explicitly.

The airflow in the dry cask system annulus is simulated using both low Reynolds k-ε model as well as k-ω SST model. The flow of helium inside the MPC is at very low Reynolds number (<100) and both the Rayleigh Number and the modified Rayleigh number are $<10^5$, suggesting that the helium flow inside the MPC is purely laminar.

Flow Resistance

During fuel storage, helium enters the MPC cells from the bottom plenum and flows upward through the open spaces in the fuel storage cells and exits through the top plenum. The top and bottom plenums are essentially open spaces to facilitate helium circulation. In the case of BWR fuel storage, a channel enveloping the fuel bundle divides the flow in two parallel paths. One flow path is through the in-channel or rodded region of the storage cell and the other flow path is in the square annulus outside the channel. In the current analysis, the channel-to-cell gap was explicitly modeled, and the porous media occupied the volume enclosed by the channel box. In the Fluent program, porous media flow resistance is modeled as follows: $\Delta P = D\mu VL$ where ΔP is the hydraulic pressure loss, D is the flow resistance coefficient, μ is the fluid viscosity, V is the superficial fluid velocity and L is the porous media length. In the analysis, the fuel storage cell length between the bottom and top plenums is replaced by porous media. To characterize the flow resistance of fuel assemblies inside the fuel channel for BWR fuel, a 3D model of GE 10x10 fuel assemblies is constructed using the Fluent CFD program. This model represents explicitly the fuel rods, water rods and grid spacers. In the 3-D flow resistance modeling, two approaches to calculate the flow resistance were used. The first approach is the pressure drop method, and the second is the shear stress method. Both methods are applied for sections without flow area changes (i.e. no contractions or expansions). Both approaches are related and should lead the same values.

Analyzed 3-D Cases

Quarter symmetry was used to minimize CPU time and effort. For the 3-D model, porous media was used inside the channel box only. Both low Reynolds k-ε and transitional k-ω SST models were used to model turbulence. Additionally, the performance of two radiation models, the Discrete ordinate (DO) and Discrete Transfer Radiation Model (DTRM) were compared.

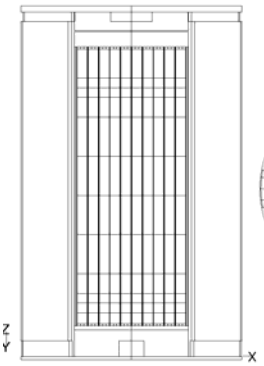

Figure 9 Cask Geometry.

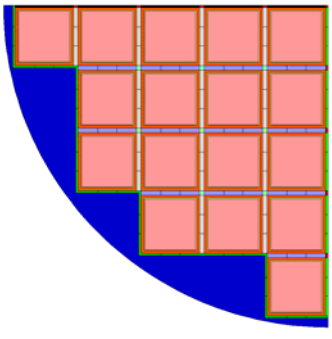

Figure 10 ¼ cross section of MPC-68 Basket using k_{eff} for channel box

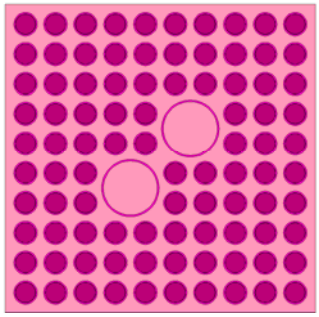

Figure 11 Two dimensional model to calculate porous media input.

Axisymmetric Model

The axisymmetric model requires several simplifications. In the most important step, the planar section of the MPC is homogenized. With each storage cell replaced with an equivalent solid square, the MPC cross section consists of a metallic grid work (basket cell walls with each square cell space containing a solid storage cell square of effective thermal conductivity, which is a function of temperature) circumscribed by a circular ring (MPC shell). In the axisymmetric model, the required simplification is carried out by replacing the thermally heterogeneous fuel basket section by an equivalent conduction-only region, using a 2-D CFD analysis. Because the rate of transport of heat in the fuel basket is influenced by radiation, which is a temperature–dependent effect, the equivalent conductivity of the fuel basket region must also be computed as a function of temperature. The MPC section consists of two discrete regions, namely, the basket region and the peripheral region. The peripheral region is the space between the peripheral storage cells and the MPC shell. This is a helium filled space surrounded by the basket walls. In particular, the effective conductivity of the storage cells is subsumed into the equivalent conductivity of the basket cross section. The fuel basket thermal modeling duly recognizes these differences by characterizing the effective conductivities in the two (planar and axial) directions. For computing the planar fuel basket conductivity, either a finite element based model such as ANSYS code or a finite volume based CFD code such as Fluent can be employed. The principal inputs to the models are the design basis fuel planar conductivities and the sandwich panel conductivities. The fuel basket axial conductivity is computed by an area weighted sum of the cladding, helium, neutron absorber and Steel (box wall and sheating) conductivities. This evaluation employs the design basis fuel and neglects fuel pellet axial conduction and axial dissipation of heat by radiation. Finally, the system is simulated as being radially symmetric having annular vents at the bottom and top with a buoyancy-induced flow in the annular space surrounding the heat generating MPC cylinder. The annular vents in the system model are porous media spaces having effective inlet and outlet duct flow resistances.

Internal circulation of helium in the sealed MPC is modeled as flow in a porous media in the fuel basket region containing the SNF (including top and bottom plenum). The basket-to-MPC shell clearance is modeled as helium filled radial gap to include the downcomer flow in the thermal model. The downcomer region consists of an azimuthally varying gap formed by the square-celled basket outline and the cylindrical MPC shell. In the Fluent axisymmetrical model, a single effective gap is used to model the downcomer region. Different turbulence models were used to analyze the flow of air and helium outside and inside the MPC respectively. Three models were used to model turbulence, transitional k-ω SST, low Reynolds k-ε and standard k-ε. Additionally, laminar flow regime was also used. Mesh requirements for the three turbulence models are different as explained in the mesh consideration and turbulence modeling in VSC-17 validation section. The transitional k-ω SST and low Reynolds k-ε require finer mesh near the wall. The dimensionless distance for cells close to the wall (y+) is close to unity for these two models. The integration is carried all the way to the wall using the finer mesh. The standard k-ε model, usually used for high Reynolds number flows, requires meshes with $y+ > 11$.

Analyzed Axisymmetrical Cases

The cases included low Reynolds k-ε, transitional k-ω SST, and standard k-ε to model the air flow turbulence. Laminar flow was also used to model air flow between the liner and the MPC walls. Laminar flow was considered because the modified Rayleigh number indicated a laminar regime as explained in [Sparrow EM et al., 1985]. For helium flow inside the MPC, even though the Reynolds and the Rayleigh numbers are too low to consider including turbulence, the effect of using the standard k-ε model was investigated. The results of two radiation models, the Discrete Ordinate (DO) model and the Discrete Transfer Radiation Model (DTRM) were compared. Two types of control volume were used, an extended control volume that included part of the ambient and a model for the dry cask only. In this control

volume (CV), the inlet and outlet ducts were boundaries but part of the computational domain. Using the extended CV and dry cask only CV, the input value for the operating density was investigated.

Results and Discussions

Axisymmetric Model

The results obtained from the extended CV case were similar to dry cask CV when the operating density in the dry cask CV was set equal to the inlet density as shown in Table 5. The similarity is very strong as shown by the values of mass flow rate, PCT, heat absorbed by air, and air exit temperature. In Table 5, as the operating density increases the air mass flow rate increases. PCT decreases due to the higher heat transfer absorbed by the higher air mass flow rate. Consequently, the air exit temperature decreases as the operating density increases. Fluent user guide suggests that the air operating density should be identical to the fluid average density. As shown in Table 5 (dry cask CV), if the operating density is equal to the average density, incorrect results are obtained. But in case of the extended CV, the average density is similar to the ambient density, as a result of the big ambient volume existing at ambient conditions. The Cases shown in Table 5 are based on the low Reynolds k-ε model to model turbulence in the air side.

Table 6 shows the PCT using low Reynolds k-ε, transitional k-ω SST, standard k-ε, and laminar regime to model turbulence in the air region of dry cask CV. In all the first four cases, laminar regime was used to model the pressurized helium inside the MPC. Table 5 shows that the low Reynolds k-ε, transitional k-ω SST lead to the same PCT, but the laminar flow regime lead to a higher PCT. Both of these turbulence models and laminar flow regime assumption predicted a PCT that exceeded the limiting temperature criteria for normal long-term storage of 400°C. As shown in Table 6, when standard k-ε was used to model turbulence in the air region, and either laminar or standard k-ε in the helium region, the resulting PCT was less than the limiting criteria of 400°C. As seen in Table 6, when standard k-ε model is used, higher air mass flow rate is induced into the cask, and more heat is absorbed from the MPC. In addition if turbulent flow is assumed inside the MPC and standard k-ε is used for modeling, even a higher heat rate is transferred to the air and lower PCT is obtained.

Table 7 shows results obtained for two cases using two different radiation models, the DO and DTRM models. In both cases, low Reynolds k-ε was used to model turbulence in the air flow and laminar regime to model helium flow inside the MPC. Both radiation models used 10 angular discretizations in each angular direction. Table 7 shows that both models performed similarly. Finally, the effect of the ambient pressure was investigated. So far, all of the cases used an ambient pressure of 1 atm. Table 8 shows results for an ambient pressure of 0.84 bars, equivalent to a site that is 1400 m above the sea level as in the case of the VSC-17 experiment site. Low Reynolds k-ε model was used to model turbulence in the air side, and laminar flow regime was assumed inside the MPC. When compared to the results obtained for the ambient pressure of 1 atm, Table 8 shows that the mass flow rate is reduced by almost 15 %, heat absorbed by the air is reduced by 6 % and the PCT increased by 17 degrees K. As shown in Table 8, the correct operating density for an ambient pressure of 0.84 bars is 0.975 kg/m^3. Table 8 shows that when the operating density is increased to 1.176 kg/m^3, the induced air mass flow rate almost doubles, heat absorbed by the air increases, PCT decreases, and the air exit temperature decreases.

3-D Model

Figure 12a and 12b show the fuel center, MPC and liner walls axial temperature distributions for two cases using low Reynolds k-ε and transitional k-ω SST to model turbulence in the air. Low Reynolds model appears to give slightly higher PCT. Both models predicted PCT that is almost 30 degrees lower than the limiting criteria of 400°C as compared to the axisymmetric model that indicated a PCT higher than the limiting criteria when the same turbulence model was used. The heat exchange between the

MPC wall and the liner is almost comparable as seen in Figure 12b. Although both turbulence models led to similar results as shown in Figure 12a and 12b, the low Reynolds k-ε is preferred as it contains the effect of gravity in the production of turbulence and its dissipation. Figure 13 shows results obtained for two cases using two different radiation models, DO and DTRM models. In both cases, transitional k-ω SST was used to model turbulence in the air flow and laminar regime to model helium flow inside the MPC. Both figures show close similarity in the final results.

Table 9 shows the dry cask thermal response when the ambient pressure is lowered to model the effect of higher altitudes on the dry cask cooling efficiency. The pressure was lowered from the ambient pressure at sea level of 1 atm to a an ambient pressure of 0.83 atm corresponding to an altitude of 1500 m as in the case of VSC-17 experiment location. As the pressure was lowered, the air mass flow rate decreased and the PCT increased due to a decrease in heat rate removal as shown in Table 9.

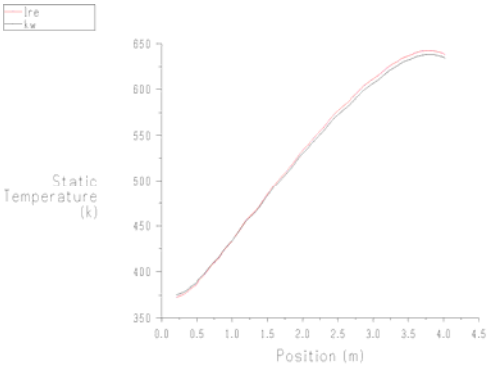

Figure 12a Fuel center temperature using 3-D model using transitional k-ω SST and low Reynolds k-ε turbulence model. (—— CFD).

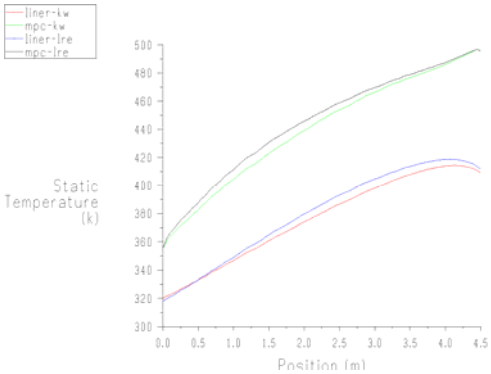

Figure 12b Liner and MPC temperature using 3-D using transitional k-ω SST and low Reynolds k-ε turbulence model. (—— CFD).

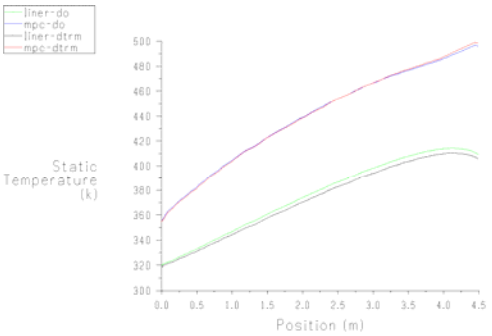

Figure 13 Liner and MPC temperature using 3-D, transitional k-ω SST turbulence for two radiation models. (—— CFD).

Type of control volume	Operating Density (kg/m^3)	PCT (Kelvin)	Air mass flow rate (kg/s)	Heat absorbed by air (Watts)	Exit temperature (Kelvin)
Dry cask	1.0352 (average)	725	0.179	19,215	408
Dry cask	1.176 (inlet)	702	0.34	22,915	367
Dry cask	1.25 (>inlet)	691	0.429	24,384	356
Extended	1.176 (inlet&average)	702	0.341	22,900	367

Table 5 Axisymmetric model using different control volumes.

Turbulence model in air passage	Turbulence model inside the MPC	Peak Clad temperature (Kelvin)	Air mass flow rate (kg/s)	Heat absorbed by air (Watts)	Air exit temperature (Kelvin)
Laminar	Laminar	718	0.292	21,032	371
Transitional k-ω	Laminar	704	0.33	22,532	367
Low Re k-ε	Laminar	702	0.34	22,915	367
Std-kε	Laminar	666	0.344	25,705	370
Std-kε	Std-kε	658	0.346	25,760	369

Table 6 Axisymmetric model using different combination of turbulence modeling.

Radiation model	Peak Clad temperature (Kelvin)	Air mass flow rate (kg/s)	Heat absorbed by air (watts)	Air exit temperature (Kelvin)
Discrete Ordinate (DO)	702	0.34	22,915	367
Discrete Transfer radiation Model (DTRM)	701	0.339	22,757	367

Table 7 Axisymmetric using different radiation models.

Operating density (kg/m3)	PCT (Kelvin)	Air mass flow rate (kg/s)	Heat absorbed by air (Watts)	Exit temperature (Kelvin)
1.176	679	0.493	26,252	353
0.975	719	0.292	21,613	374

Table 8 Axisymmetric model for different operating density at an ambient pressure of 84000 Pa

Ambient Pressure (atm)	Operating density (kg/m^3)	Peak cladding Temperature (Kelvin)	Air mass flow rate (kg/s)	Heat absorbed by air (Watts)	Exit Temperature (Kelvin)
1	1.176	645	0.338	24,152	369
0.83	0.975	659	0.288	22,856	376

Table 9 3-D analysis using low Re k-ε turbulence model, and channel porous media evaluated at two different ambient pressures

CONCLUSIONS

This paper describes the application of the Fluent commercial CFD code to model momentum and energy conservation in a dry cask. As a first step, temperature measurements for the VSC-17 spent fuel storage cask undertaken by Idaho National Lab (INL) were used to validate the 3-D CFD model. In the validation part, the flow in the air channel is found to be in the transitional region of turbulence. Only turbulence models that are able to deal with this region of the flow regime should be used to perform the analysis. Among the available turbulence models in Fluent, the transitional k-ω SST and low Reynolds k-ε models were able to predict the experimental data. These models require finer mesh near the wall. The low Reynolds k-ε is preferred because it includes the effect of gravity in the production and dissipation of turbulent kinetic energy. The laminar flow regime overpredicts the PCT and is not appropriate to analyze the air flow. The standard k-ε model is not suitable to model the air flow because it overpredicts the heat transfer from the fuel rods to the air. The flow inside the MPC is laminar. Only laminar flow is appropriate to model flow inside the MPC. When pressure boundaries are used at the inlet and outlet ducts of the dry cask, the operating density should be evaluated at the inlet conditions of temperature and pressure.

After the validation step, a dry cask system holding 68 BWR assemblies is modeled using two approaches. One approach used axisymmetrical representation of the dry cask and the second used a more realistic 3-D model. Based on the predicted PCT the axisymmetric model is more conservative than the 3-D models. In the axisymmetric approach, when standard k-ε model was used for air flow and laminar regime was used for helium inside the MPC, PCT criterion was satisfied. Additionally, when standard k-ε model was used to model both air and helium flows, even lower PCT was obtained than the above. The lower Reynolds turbulence model as well as the transitional k-ω were found equivalent, but the former is suggested for modeling because this model contains the effect of gravity in the production turbulent kinetic energy and its dissipation. The effect of gravity is very important in modeling flow and heat transfer in dry cask which is driven by buoyancy forces. The performance of the two chosen radiation models, DTRM and DO, were identical and gave close results in the axisymmetrical model.

In the 3-D model, low Reynolds turbulence k-ε model as well as the transitional k-ω were found equivalent to each other. But as mentioned above, the low Reynolds k-ε is preferred, because it includes the effect of gravity in the turbulent kinetic energy and its dissipation. This is important, considering that the flow in the dry cask is driven by buoyancy forces that depend on the density difference and gravity. When the inlet and outlet ducts to the dry cask are used as pressure boundaries, the operating density should be evaluated at the inlet conditions. The performance of the two chosen radiation models, DTRM and DO, were identical and gave close results. For higher elevations, ambient pressure decreases, less air mass flow rate is available to cool the dry cask, and a higher PCT is obtained.

REFERENCES:

1 McKinnon MA, RE Dodge, RC Schmitt, LE Eslinger, and G Dineen, 1992, "Performance Testing and Analyses of the VSC-17 Ventilated Concrete Cask". TR-100305, Electric Power Research Institute, Palo Alto, California.

2 Fluent User Guide Version 6, Fluent Inc, New Hampshire, 2006.

3 E. M. Sparrow and L. F. A. Azevedo "Vertical-channel natural convection spanning between the fully-developed limit and the single-plate boundary-layer limit", International Journal of Heat and Mass transfer, Vol.28, No.10, pp.1847-1857, 1985.

4 E. M. Sparrow, and A. L. Loeffler, JR "Longitudinal laminar flow between cylinders arranged in regular array", A.I.Ch.E. Journal, Volume 5, No.3, pp325-330, 1959.

5 "Cladding Considerations for the Transportation and Storage of Spent Fuel," Interim Staff Guidance -11 (ISG-11), Revision 3, USNRC, Washington D.C.

6 NUREG-1536, "Standard Review Plan for Dry Cask Storage Systems," USNRC, January 1997, Washington DC.